

✓
1N09
203570
18 P

Flow Quality Studies of the NASA Lewis Research Center Icing Research Tunnel Diffuser

E. Allen Arrington
Sverdrup Technology, Inc.
Lewis Research Center Group
Brook Park, Ohio

and

Mark T. Pickett and David W. Sheldon
National Aeronautics and Space Administration
Lewis Research Center
Cleveland, Ohio

January 1994

(NASA-TM-106311) FLOW QUALITY
STUDIES OF THE NASA LEWIS RESEARCH
CENTER ICING RESEARCH TUNNEL
DIFFUSER (NASA) 18 p

N94-23091

Unclass

G3/09 0203570



FLOW QUALITY STUDIES OF THE NASA LEWIS RESEARCH CENTER

ICING RESEARCH TUNNEL DIFFUSER

E. Allen Arrington
Sverdrup Technology, Inc.
Lewis Research Center Group
Brook Park, Ohio 44142

and

Mark T. Pickett and David W. Sheldon
National Aeronautics and Space Administration
Lewis Research Center
Cleveland, Ohio 44135

Abstract

The purpose of this study was to document the airflow characteristics in the diffuser of the NASA Lewis Research Center Icing Research Tunnel and to determine the effects of vortex generators on the flow quality in the diffuser. The results of this study were used to determine how to improve the flow in this portion of the tunnel so that it can be more effectively used as an icing test section and to improve overall tunnel efficiency. The demand for tunnel test time and the desire to test models that are too large for the test section were two of the drivers behind this diffuser study. For all vortex generator configurations tested, the flow quality was improved.

Several types of data were collected to characterize the flow in the diffuser with and without vortex generators. Surveys of total and static pressure and total temperature were made near the diffuser exit using three rakes that were positioned in several configurations. Vortex generators (VG's) were mounted near the inlet of the diffuser. The flow-field surveys were made with the standard tunnel configuration (no diffuser vortex generators installed) and two vortex-generator configurations (that is, two vortex-generator axial locations). The boundary-layer thickness was measured near the inlet of the diffuser to aid in the placement of the vortex generators. Axial static-pressure distributions were recorded along each wall of the diffuser (from the test section inlet to the diffuser exit) in order to determine the presence and location of separated flow areas in the diffuser. Flow visualization using smoke traces was performed for the same purpose.

The tests revealed that the vortex generators in general had a slight positive effect on the flow quality in the diffuser but also decreased the Mach number at the diffuser exit. Mach number distributions at the diffuser exit show that the vortex generators decrease the centerline Mach number: at a test section Mach number of 0.39 (300 mph),

the Mach number measured at the center of the diffuser exit plane is 0.16 without vortex generators, 0.14 with the vortex generators at the downstream station, and 0.11 with the vortex generators at the upstream station. The vortex generators increased useable test area in the diffuser and decreased the pressure gradients over the survey plane. These effects on the diffuser flow field were recorded for both vortex generator configurations, although greater effects were realized with the vortex generators at the upstream station. The operating efficiency of the tunnel was only minimally improved by the vortex generators: drive fan speed decreased only 0 to 5 rpm with the vortex generators installed.

Introduction

Flow-field surveys have been made in the diffuser of the NASA Lewis Research Center's Icing Research Tunnel (IRT) in order to determine the flow quality with and without vortex generators. The purpose of these studies was to document the existing diffuser flow quality and to assess the effect of vortex generators on the flow field in the diffuser and on overall tunnel performance. The vortex generator design and configurations were based on the successful techniques used in a similar NASA wind tunnel, the NASA Ames 7- by 10-ft subsonic wind tunnel. This design was selected because it could be quickly implemented at low cost and could provide the required information on the gross effects of VG's on the diffuser flow field. No attempt was made to optimize the vortex generator configuration during the study nor to design vortex generators specifically for this application. The intent of the study was to determine the general effects of vortex generators on the IRT. Additional information on the IRT diffuser flow quality is found in Ref. 1.

This report describes the measurements made, instrumentation used, and data obtained in support of the diffuser flow quality studies.

The authors would like to thank Richard R. Burley of NASA Lewis for providing the information concerning diffuser design criteria and specific analyses of the IRT diffuser. This information is found in the Diffuser design section of the current work.

Description of Facility

The NASA Lewis IRT is a closed-loop atmospheric tunnel with rectangular cross sections (Fig. 1). The airflow is driven by a 25-ft diameter, 12-blade fan that is powered by a 5000-hp electric motor. The tunnel test section is 6 ft high, 9 ft wide, and 20 ft long. The velocity in an empty test section can be varied from 50 to 300 mph. Eight horizontal spray bars, located upstream of the test section, inject atomized water into the airflow to create icing conditions (no icing conditions were studied in these tests). The inside dimensions of the tunnel at the survey plane (also shown in Fig. 1.) are 16.58 ft wide and 13.58 ft high. The diffuser is 81.5 ft long, its area ratio is 4.17, and its angle is approximately 5.3° . Tunnel station zero is located at the inlet of the test section. A complete description of the facility is contained in Ref. 2.

Instrumentation and Test Hardware

Flow-Field Surveys

Several types of flow-sensing probes and rakes were used in the flow quality studies, including total- and static-pressure probes, thermocouples, wall static-pressure taps and boundary-layer rakes. Each probe type, its associated support system, and the locations used are described in the following sections:

Diffuser exit plane surveys.—Three rakes were used to map the flow field at the diffuser exit: a vertically oriented rake and two corner-mounted rakes. The following instrumentation was mounted to each of these rakes:

Vertical survey rake

- 19 total pressure probes
- 16 static pressure probes
- 16 total temperature probes

Corner survey rakes

- 7 total pressure probes
- 5 static pressure probes
- 5 total temperature probes

Figures 2 and 3 show the probe positions for each rake, and Fig. 4 shows a typical test setup. To completely map

the flow field, the vertical rake was located at five positions across the survey plane, and the corner rakes were placed in each corner of the survey plane. Figure 5 shows the location of the probes at the survey plane. The total-pressure probe heads were of a standard design with a 60° chamfer to allow for flow angularity. The static-pressure probes were composed of four static-pressure taps connected to a common manifold. The total temperature was measured using aspirated thermocouples. The measurement ports of the total-pressure, total-temperature, and static-pressure probes were all located in the same plane, although the probes were staggered along the span of the rake. The total-pressure probes were mounted through the chord line of the rake body. The static-pressure probes were mounted through the upper surface of the rake, and the thermocouples through the lower surface of the rake body. Details of the instrumentation used are given in Fig. 6.

Axial static-pressure distribution.—The static-pressure distribution along each of the tunnel walls was measured by means of improvised wall static taps. The wall taps were made using soft rubber instrumentation tubing belts. Each belt is composed of 10 individual tubes. A hole exposed to the flow was cut through the wall of each tube to sense the static pressure. Several of these tubing strips were taped to the test section and diffuser walls. By staggering the position of the static tap locations for each tube, the axial static-pressure distribution through the test section and diffuser was measured. The belts were installed at the vertical centerline of the test section and diffuser and extended from the inlet of the test section to the diffuser exit.

Boundary-layer measurements.—One boundary-layer rake was used to determine the thickness of the boundary layer at the upstream vortex generator station with the vortex generators installed. The rake was composed of 15 total-pressure probes, arrayed to provide more information nearer to the tunnel floor. Figure 7 shows the instrumentation layout of the rake used to measure the boundary-layer thickness in the diffuser.

Vortex generators.—The vortex generator setup is shown in Fig. 8. Each VG is made of sheet metal bent into a circular arc and welded to a mounting plate. The VG's were bolted to the tunnel structure. The VG's have a span (height) of 11 in. and a chord of 14 in. with a $5/8$ -in. camber (straight radius) and are set at an angle of attack of 14° (Fig. 8(c)). The VG's were modeled after VG's used in the NASA Ames 7- by 10-ft wind tunnel.³ Four pairs of VG's were used, one pair on each surface of the diffuser. In the downstream configuration, the VG's were located at tunnel station 35 (15 ft downstream of the test section exit); in the upstream configuration, they were located at tunnel station 26.33 (6 ft 4 in. downstream of the test section exit). The positions of the VG's at the axial stations are given in Fig. 8.

Data system.—The standard tunnel data system was used to record the pressure measurements made during these studies. The tunnel data system consists of a VAX-based data-acquisition system and an electronically scanned pressure (ESP) system. For these tests, 5-psid ESP modules were used. The modules were accurate to within 0.0035 psia.

Flow Visualization

In order to determine whether the flow in the diffuser remained attached to the tunnel walls, flow visualization was used. Smoke generators were attached to the north test section wall and ignited at a test section airspeed of 100 mph. The smoke traces were observed and recorded from the north side of the diffuser exit. The path of the smoke traces was recorded using a hand-held video camera. The vortex generators were not installed in the tunnel during the flow visualization test. The smoke generators were small, electrically ignited canisters that produced 100 000 ft³ of smoke over a 5-min period. The smoke generators were approximately 8 in. long and 1 in. in diameter.

Test Procedures

Figure 1 shows the locations of the survey planes and the vortex generator stations in the tunnel. The procedure was to set the diffuser rake positions and make three runs (velocity sweeps) covering the operating range of the facility. The VG configuration was changed for each run (one run without the vortex generators installed and one run each with vortex generators installed at the upstream and downstream stations). This procedure was repeated for each of the five vertical rake positions described previously. In this manner, the flow field at the diffuser exit was mapped and the effects of the vortex generators on the flow field were documented. A similar method was used in collecting the diffuser axial static-pressure distributions.

Discussion of Results

Diffuser surveys.—Total-pressure profiles measured along the vertical centerline of the diffuser exit are shown in Fig. 9 for corresponding to test section velocities V_{ts} of 100, 200, and 300 mph for each VG configuration. In this figure, the total pressures measured at the diffuser exit have been nondimensionalized by the test-section total pressure. The VG's have the greatest effect on the flow at a V_{ts} of 300 mph. The upstream VG's produced the greater difference from the baseline (no VG's). Both VG configurations had a greater effect on the flow near the ceiling of the diffuser than near the floor. For the baseline configuration, the total pressure is greater along the diffuser floor than at the ceiling. Both upstream and downstream VG configurations

increase the total pressure near the boundaries such that the total pressure measured near the ceiling and floor are approximately equal. The total pressure at the center of the diffuser exit was reduced approximately 4 percent for the downstream configuration and about 6 percent for the upstream configuration at $V_{ts} = 300$ mph. Similar trends are seen at the other test section velocities, but the magnitude of the changes is reduced.

Figures 10 to 13 show contour plots of total and static pressure, total temperature, and Mach number at the diffuser exit for each VG configuration and each test section velocity (of 100, 200, and 300 mph). For these contour plots, the total and static pressure and total temperature measured at the diffuser exit have been divided by the corresponding test section settings to account for differences in day-to-day test conditions. Test section flow conditions and general trends and results from the diffuser surveys are listed in Table 1.

The vortex generators had a greater effect on the diffuser exit flow field at conditions corresponding to the highest test section velocities. The upstream VG configuration produced a better total-pressure distribution over the survey plane. At $V_{ts} = 300$ mph, the total pressure and Mach number at the diffuser survey plane were decreased by the action of the VG's, the uniformity of the flow field at the survey plane was improved by the use of the VG's. As a means of comparison, the core size of the survey plane was estimated for each VG configuration. The core is defined as the area in which the selected flow-field parameter varies less than 0.5 percent from the maximum value. For the total pressure surveys, the core area was at the center of the survey plane. For the baseline configuration at $V_{ts} = 300$ mph, the core size was approximately 11 percent of the total area and increased to 27 percent and to 34 percent for the downstream and upstream configurations, respectively. The overall total-pressure variation and gradient over the survey plane were decreased by the use of the vortex generators. Similar effects were seen in the Mach number data (Fig. 13), although the increase in core size (not shown in table) was not as significant as in the total-pressure data. The static pressure profiles were fairly flat regardless of the VG configuration, but some improvement was noted for the upstream VG configuration. Similar effects were noted for V_{ts} of 100 and 200 mph, although the magnitude of these effects was less at these velocities.

Axial static-pressure distributions.—The static pressure distributions along both the north and south diffuser walls are given in Fig. 14. The static pressures were measured along the tunnel wall from the test section inlet to the exit of the diffuser using the static-pressure-tap strips previously described. The baseline configuration data show a fairly flat static-pressure distribution through the test section and a smoothly increasing profile as the flow enters the diffuser. The slight pressure discrepancy in the profile along the north wall at tunnel station 80 is due to a wall plate that

extends into the flow field. This discrepancy is exaggerated by the presence of the vortex generators as shown in Figs. 14(b) and (c). The presence of the vortex generators is also apparent in the pressure distributions at tunnel station 26.33 (configuration two) and station 35 (configuration one). Comparison of the static-pressure distributions show that the VG's decrease the static pressure in the test section but increase it at the exit of the diffuser. This effect is more pronounced for the upstream VG configuration. Data from the diffuser exit survey tests support this observation. Note that this variation could also be due to differences in operating conditions between the three runs required to collect these data. The data do not indicate the presence of flow separation from either diffuser wall over the operating range of the tunnel. The difference in the static pressure levels between the north and south tunnel walls is caused by day-to-day changes in the atmospheric conditions (north and south wall data were collected on different days).

Boundary-layer rake.—Measurements of the boundary-layer thickness were made on the diffuser floor at the upstream VG station with the vortex generators installed. The boundary-layer rake was mounted along the diffuser centerline such that it was positioned between the two VG's mounted on the diffuser floor. The total-pressure distributions recorded using this rake are presented in Fig. 15. These data showed that at a test section velocity of 50 mph, the boundary layer at this location in the diffuser was 4.2 in.; at 150 mph, the boundary layer thickness was 11.0 in.; and above 200 mph, the boundary layer thickness at the upstream VG station was 15.6 in.

Flow visualization.—Only limited information on the flow in the diffuser was gleaned from the flow visualization test. The test setup and procedures required to ignite the smoke generator lead to a large volume of smoke being introduced into the flow field before the test condition was set. The flow visualization test did show that there is a great deal of flow mixing in the diffuser along the diffuser wall. Figure 16 is a sketch of the approximate path of the smoke traces recorded during the flow visualization test. The smoke traces indicated the areas of flow detached from the north diffuser wall at approximately tunnel station 80 (1/2 to 2/3 of the diffuser length) at a test section velocity of 100 mph. As noted above, the static-pressure distributions made along the diffuser walls did not indicate flow separation in the diffuser. The detached flow shown during the flow visualization test could have been caused in part by the presence of the two-man film/observation team at the diffuser exit.

Diffuser design.—Three criteria were used to determine the effectiveness of the diffuser design: equivalent conical angle associated with the geometric area ratio, one-dimensional total-pressure recovery, and one-dimensional static pressure recovery. The equivalent conical angle (approximately 6°) and the area ratio (4.17) suggest that

there might be no significant separation based on the stability data available for diffusers.⁴ Based on this analysis and the IRT diffuser equivalent conical angle and area ratio, the IRT diffuser is defined as "successful" (i.e., flow is attached almost everywhere and the exit profile is fairly uniform with low turbulence intensity). The wall static-pressure distribution supports this as there were no indications of flow separation along the diffuser walls. The ideal one-dimensional static pressure recovery⁵ is approximately 1.1026 for a Mach number of 0.395. The wall static pressure recovery is 1.101 at $M_{ts} = 0.395$ (Fig. 13), which suggests that the diffusion process is quite effective at 0.9985 (1.101/1.1026). The estimated one-dimensional total-pressure recovery⁶ at a Mach number of 0.395 is 0.99.

Drive fan efficiency.—Figure 17 shows the drive fan speed required to set empty test section velocities without VG's installed in the diffuser. Figure 18 shows the difference in fan speed for the two VG's configurations compared with the baseline configuration. These data show that there is very little reduction in fan speed over the operating range of the tunnel using the vortex generators. The downstream VG configuration reduced the required fan speed a maximum of 5 rpm at test section velocities of 150 and 250 mph. The upstream VG configuration had a smaller effect on fan speed. Most of the data show little or no change (0 to 3 rpm) in fan speed. Experimental data show that the VG's will only increase test section velocity by 2 to 3 mph.

Conclusions

Flow quality studies were conducted in the diffuser section of the NASA Lewis Research Center Icing Research Tunnel with and without vortex generators to determine their effect on flow quality in the diffuser and on overall tunnel efficiency. Pressure and temperature surveys were made at the diffuser-exit plane to determine the effect of vortex generators on the flow field. Two vortex generator configurations were used in the tests. It was found that the vortex generators do improve the flow quality in the diffuser. The VG's decrease the Mach number and total pressure at the exit plane and produce more uniform total- and static-pressure distributions. The upstream VG configuration had the better effect on the overall flow quality by producing more uniform pressure profiles and less severe gradients over the survey plane. Total-pressure and Mach number at the diffuser exit survey plane were reduced more by the upstream VG configuration. Axial static pressure measurements made from the test section inlet to the exit of the diffuser along both walls showed no indication of flow separation within the diffuser. These measurements also showed that the VG's have very little effect on the wall static pressure distribution in the diffuser. The VG's do increase the static pressure levels slightly but the overall shape of the distribution is the same. The vortex generators caused only a minimal gain in the operating efficiency of

the tunnel. The fan speed was reduced 0 to 5 rpm for tunnel runs with the vortex generators installed.

Vortex generators have proven effective in the diffusers of other wind tunnel facilities. These studies have shown that VG's improve the flow quality at the diffuser exit and that the vortex generator design and configurations tested have a minimal effect on the tunnel efficiency (as seen in the slight reduction in fan speed). Experimental results and a review of the diffuser geometry indicate that there is presently good flow quality in the IRT diffuser. This, coupled with the fact that the effectiveness of vortex generators will be degraded in icing conditions,¹ indicate that it is probably not warranted to optimize the vortex generator design for use in the IRT diffuser.

References

¹Addy, H.E.; and Kerth, Jr., T.G.: Investigation of the Flow in the Diffuser Section of the NASA Lewis Icing Research Tunnel; NASA TM-102087, AIAA-89-0755, Jan. 1989.

²Soeder, R.H.; and Andracchio, C.R.: NASA Lewis Icing Research Tunnel User Manual. NASA TM-102319, 1990.

³Wadcock, A.J.: The NASA Ames 7 ft x 10 ft Wind Tunnel—Present Flow Quality and Recommendations for Improvement. Report 8705, Analytical Methods Inc., Redmond, WA, July 1987.

⁴Mehta, R.D.: The Aerodynamic Design of Blower Tunnels with Wide-Angle Diffusers. Progress in Aerospace Sciences, vol. 18, no. 1, 1977, pp. 59-120.

⁵Henry, J.R.; Wood, C.C.; and Stafford, W.W.: Summary of Subsonic Diffuser Data. NACA RM-L56F05, 1956.

⁶Sovran, G.; and Klomp, E.D.: Experimentally Determined Optimum Geometries for Rectilinear Diffusers with Rectangular, Conical or Annular Cross-Section. Fluid Mechanics of Internal Flow, Proc. of a Symposium, G. Sovran, ed., Elsevier Publishing Co., New York, 1967, pp. 270-312.

¹The vortex generators could be heated to prevent ice from forming, but this would affect the icing cloud in the diffuser (this is only a consideration if the diffuser is being used as the test chamber).

TABLE 1.—SUMMARY OF TEST SECTION CONDITIONS AND DIFFUSER EXIT SURVEY PLANE RESULTS FOR EACH TEST CONFIGURATION

| TABLE 1.—SUMMARY OF TEST SECTION CONDITIONS AND DIFFUSER EXHIL SURVEY PLANE RESULTS FOR EACH TEST CONDITION | | | | | | | | | | | | | |
|---|-----------------------------|----------------------------------|-----------------------------------|-------------------------------------|---------------------------|----------------|--------------------------|---------------------------|----------------|-----------------------|----------------|---------------------------|-------|
| VG configu- ration | Test section setting | | | | Maximum $P_o/P_{o,ts}$ | Vari- ation | Core size, percent | Maximum $P_s/P_{s,ts}$ | Vari- ation | Maximum M/M_{ts} | Vari- ation | Maximum $T_o/T_{o,ts}$ | |
| | Mach number, M_{ts} | Total pressure, $P_{o,ts}$ | Static pressure, $P_{s,ts}$ | Total temperature, $T_{o,ts}$ | | | | | | | | | |
| $V_{ts} = 300$ mph | | | | | | | | | | | | | |
| Baseline | 0.395 | 14.338 | 12.857 | 534.6 | 1.000 | 0.018 | 11 | 1.092 | 0.003 | 0.160 | 0.120 | 1.002 | 0.004 |
| Upstream | .394 | 14.319 | 12.864 | 534.7 | .996 | .012 | 27 | 1.094 | .003 | .140 | .080 | 1.002 | .003 |
| Downstream | .395 | 14.165 | 12.720 | 535.7 | .994 | .008 | 34 | 1.096 | .002 | .120 | .060 | 1.002 | .003 |
| $V_{ts} = 200$ mph | | | | | | | | | | | | | |
| Baseline | 0.263 | 14.334 | 13.661 | 524.7 | 1.000 | 0.008 | 26 | 1.0402 | <0.002 | 0.100 | 0.060 | 1.001 | 0.002 |
| Upstream | .264 | 14.332 | 13.656 | 524.1 | .998 | .005 | 52 | 1.0400 | .001 | .090 | .050 | 1.002 | .004 |
| Downstream | .264 | 14.184 | 13.516 | 524.3 | .997 | .004 | 100 | 1.0400 | .001 | .080 | .030 | 1.001 | .002 |
| $V_{ts} = 100$ mph | | | | | | | | | | | | | |
| Baseline | 0.131 | 14.346 | 14.175 | 523.0 | 1.000 | 0.002 | 100 | 1.009 | <0.001 | 0.050 | 0.030 | 1.002 | 0.002 |
| Upstream | .131 | 14.341 | 14.171 | 522.2 | .999 | .002 | 100 | 1.009 | <.001 | .050 | .030 | 1.003 | .005 |
| Downstream | .131 | 14.196 | 14.028 | 521.1 | .999 | .001 | 100 | 1.010 | <.001 | .040 | .020 | 1.001 | .002 |

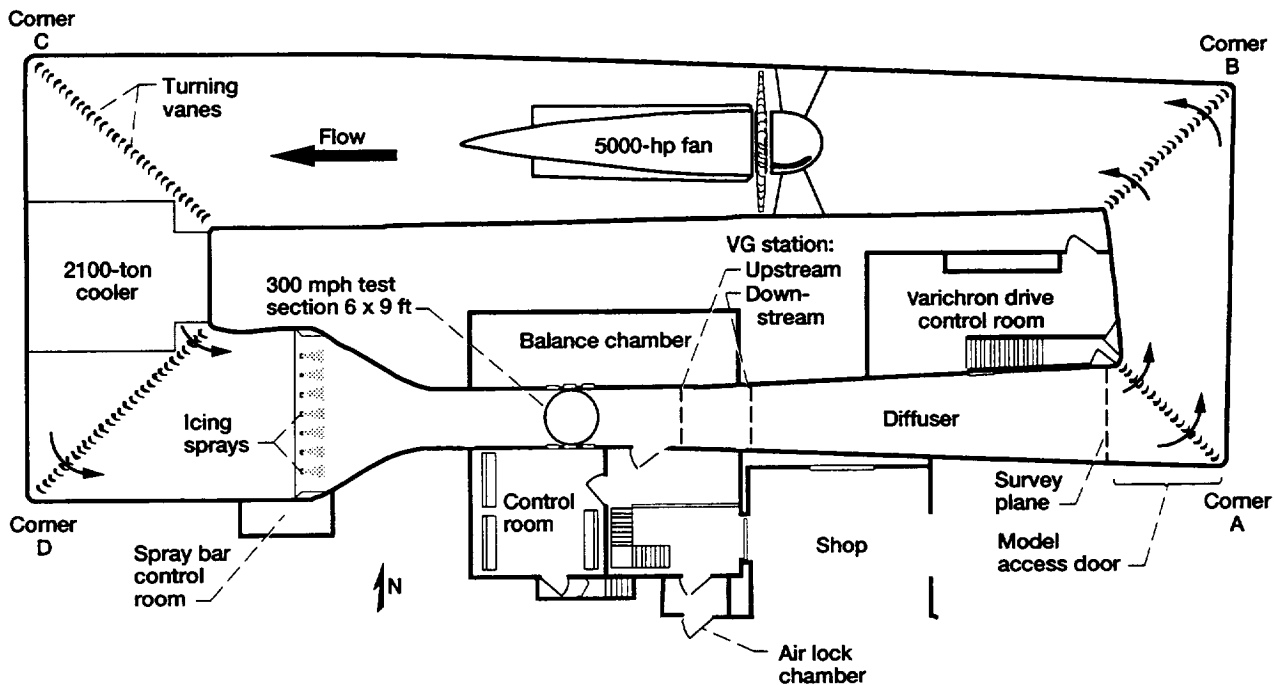


Figure 1.—Plan view of Icing Research Tunnel, shop, and control room, showing diffuser exit plane survey location.

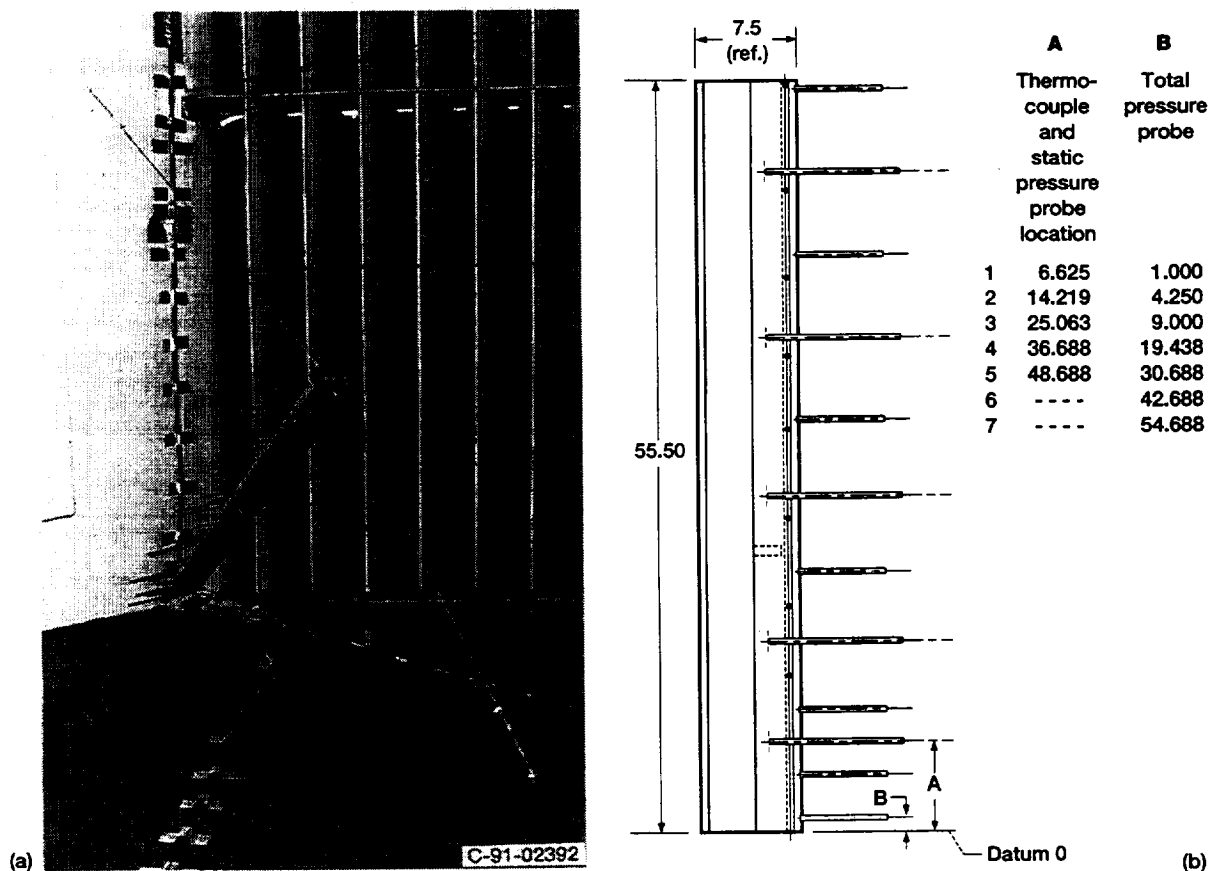


Figure 2.—Typical corner rake used in diffuser flow surveys. (Dimensions are in inches. See fig. 5 for rake positions.)
 (a) Corner rake mounted at position 4 (north-floor). (b) Instrumentation layout.

| Probe Number | A1 T/C and P _s probe location | B1 P _o probe location | A2 T/C and P _s probe location | B2 P _o probe location |
|--------------|--|--|--|--|
| 1 | 6.258 | 2.300 | 6.438 | 2.500 |
| 2 | 11.613 | 4.550 | 11.813 | 4.750 |
| 3 | 19.488 | 7.925 | 19.688 | 8.125 |
| 4 | 28.175 | 15.300 | 28.378 | 15.500 |
| 5 | 38.675 | 23.675 | 38.875 | 23.875 |
| 6 | 50.675 | 44.675 | 50.875 | 32.875 |
| 7 | 62.675 | 56.675 | 62.875 | 44.875 |
| 8 | ---- | 68.675 | 74.875 | 56.875 |
| 9 | ---- | ---- | 86.875 | 68.875 |
| 10 | ---- | ---- | ---- | 80.875 |

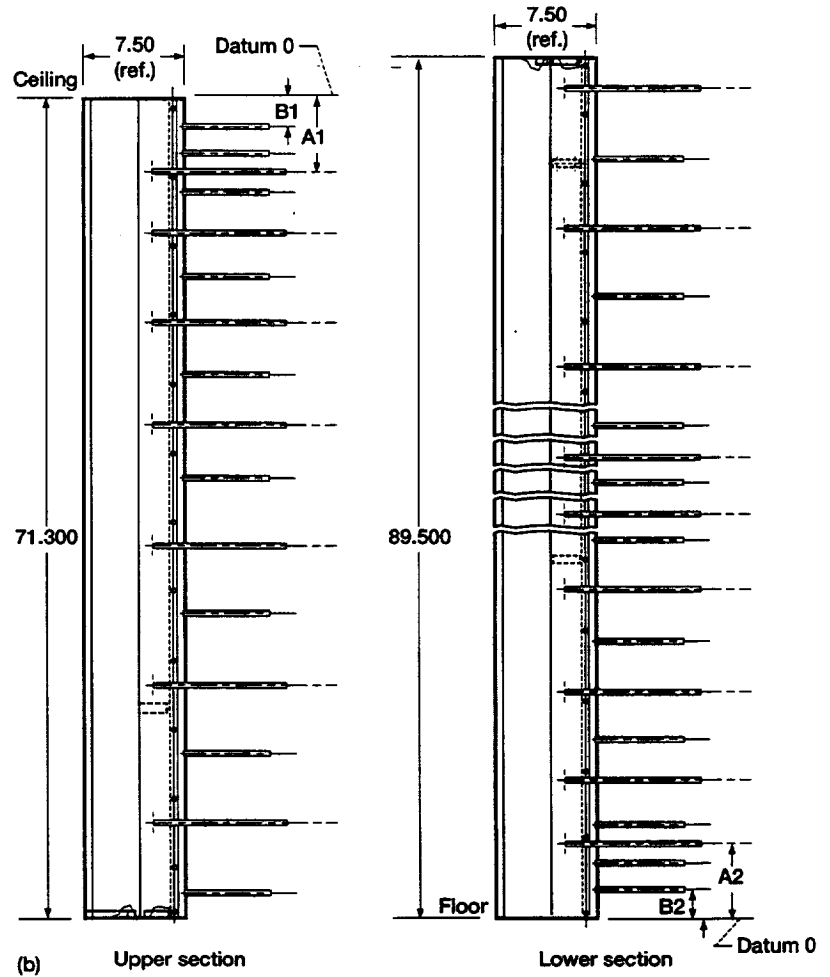
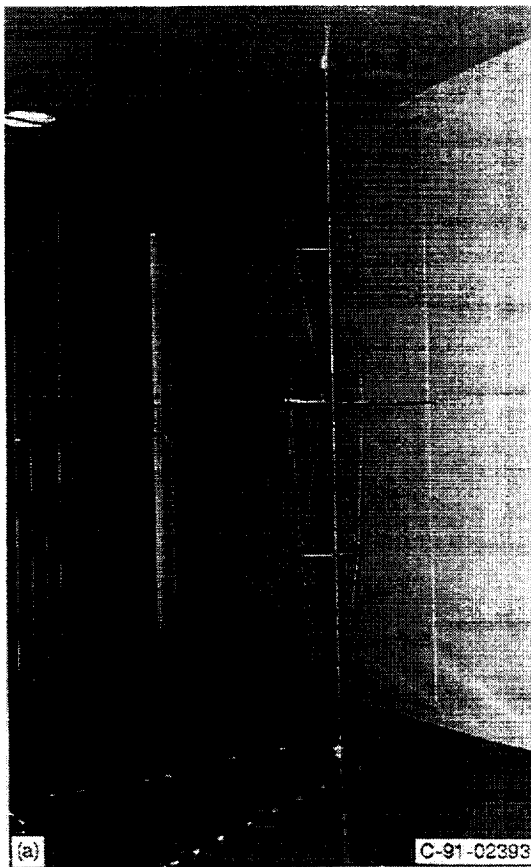


Figure 3.—Typical vertical rake used in diffuser exit survey. (Dimensions are in inches. See fig. 5 for rake positions.) (a) Vertical survey rake mounted in vertical rake position 5. (b) Vertical rake instrumentation layout.

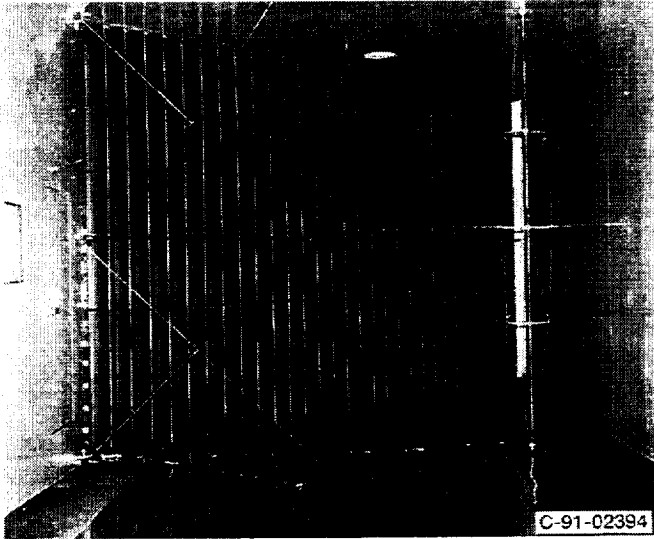


Figure 4.—Typical test set up used during diffuser exit surveys. Two corner rakes and one vertical rake were used to map the flow field at the diffuser exit. The corner rakes are in positions 1 (upper north wall) and 4 (lower north wall) and the vertical rake is at position 5 (nearest south wall).

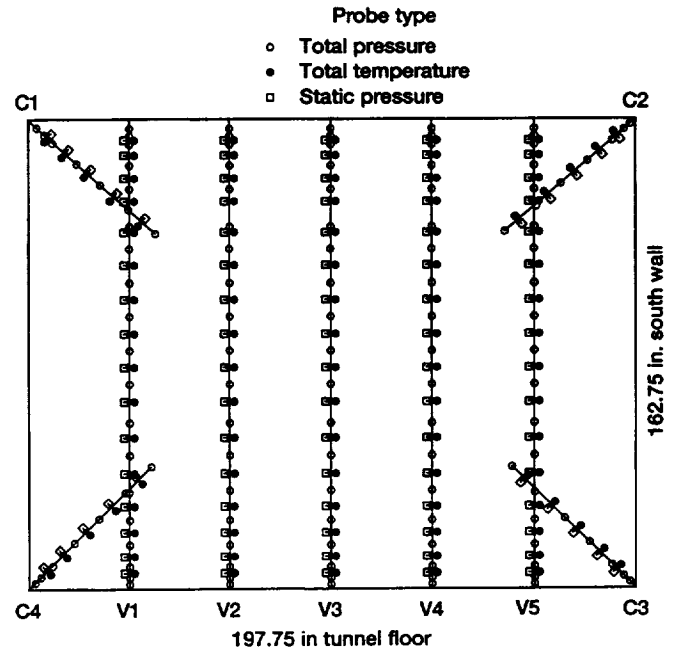


Figure 5.—Rake matrix layout and probe head locations.

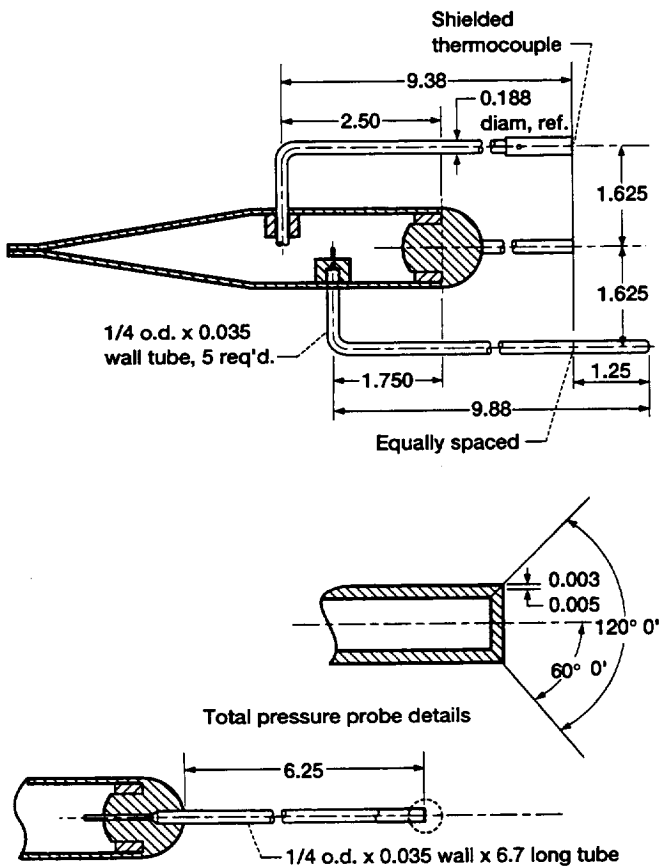


Figure 6.—Cross section of diffuser survey rakes showing probe details. Rake thickness = 1.25; Chord = 7.53. (All dimensions in inches.)

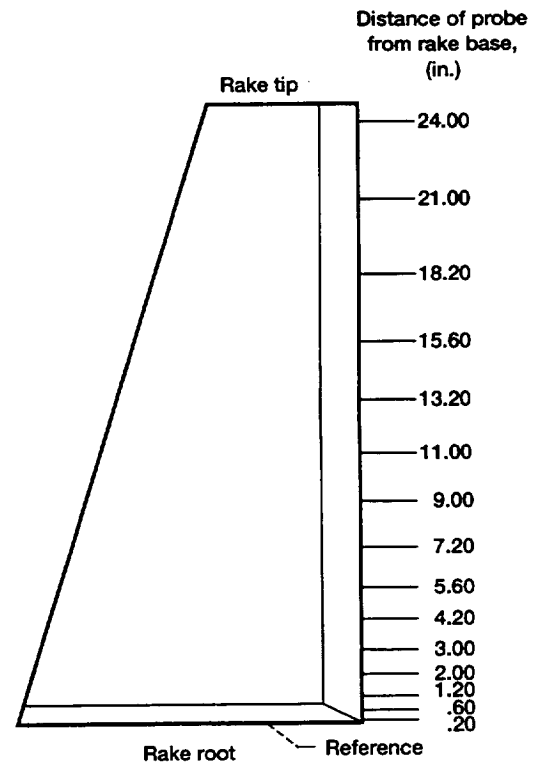
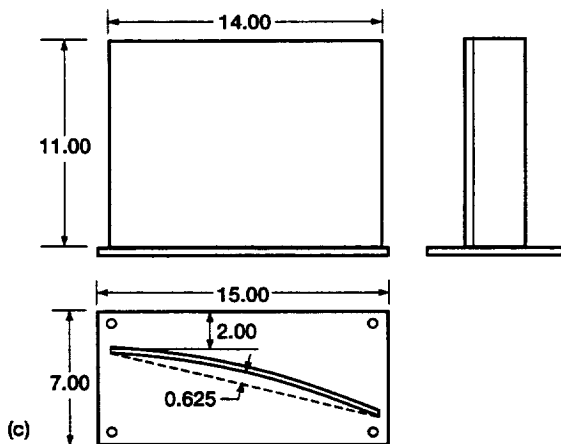
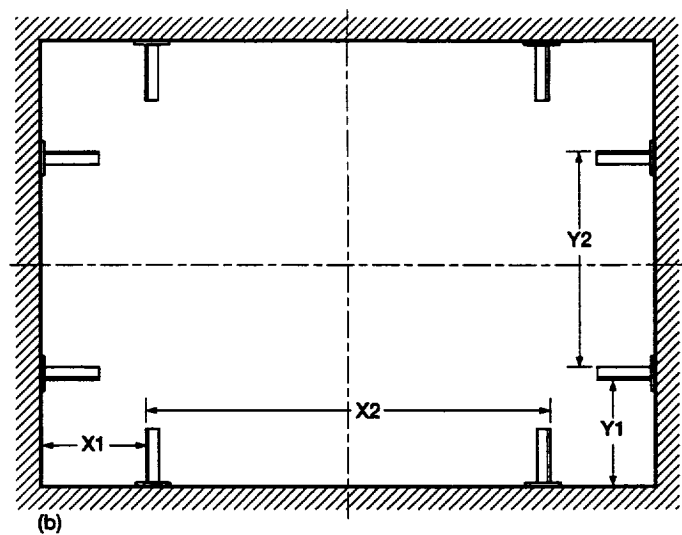


Figure 7.—Instrumentation layout of boundary layer rake used during diffuser flow quality studies.



| | Downstream VG con- figuration | Upstream VG configuration |
|--------|-------------------------------------|------------------------------|
| Width | 123 | 114 |
| X1 | 21.25 | 24.25 |
| X2 | 80.5 | 65.6 |
| Height | 88.75 | 79.25 |
| Y1 | 21.0 | 24.0 |
| Y2 | 46.75 | 31.25 |

Figure 8.—Vortex generator dimensions and configurations. (a) Setup near diffuser inlet (upstream configuration). (b) Positions. (c) Typical details. (Material thickness = 0.25 in.)

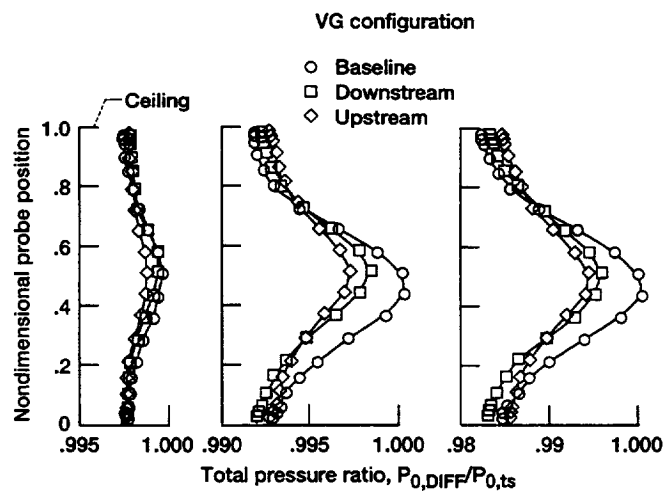


Figure 9.—Total-pressure distribution measured at diffuser exit for each vortex generator configuration (vertically oriented rake).
(a) $V_{ts} = 100$ mph. (b) $V_{ts} = 200$ mph. (c) $V_{ts} = 300$ mph.

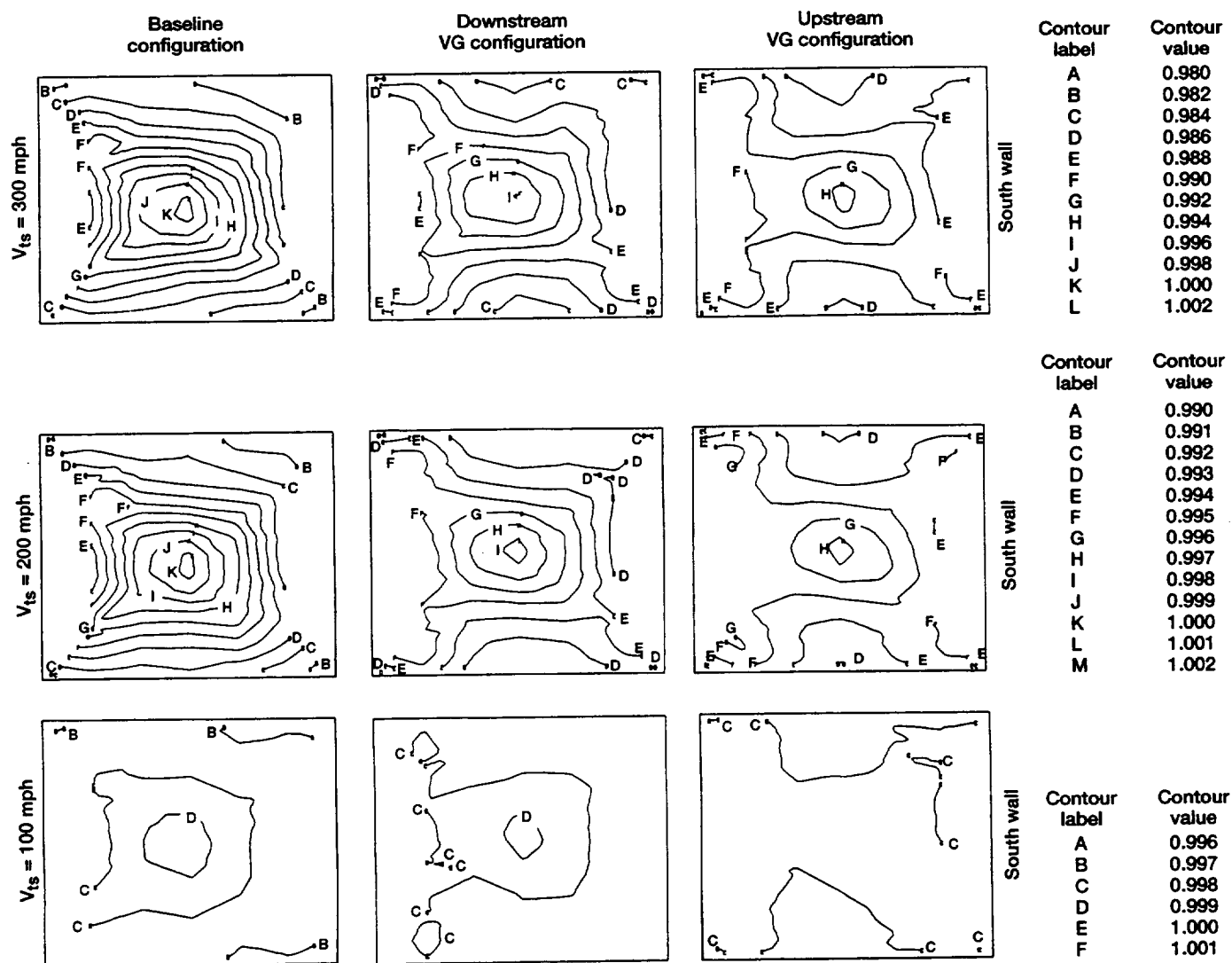


Figure 10.—Contour plots of total pressure survey data collected at the diffuser exit normalized by test section total pressure ($P_0/P_{0,ts}$). (Downstream views.)

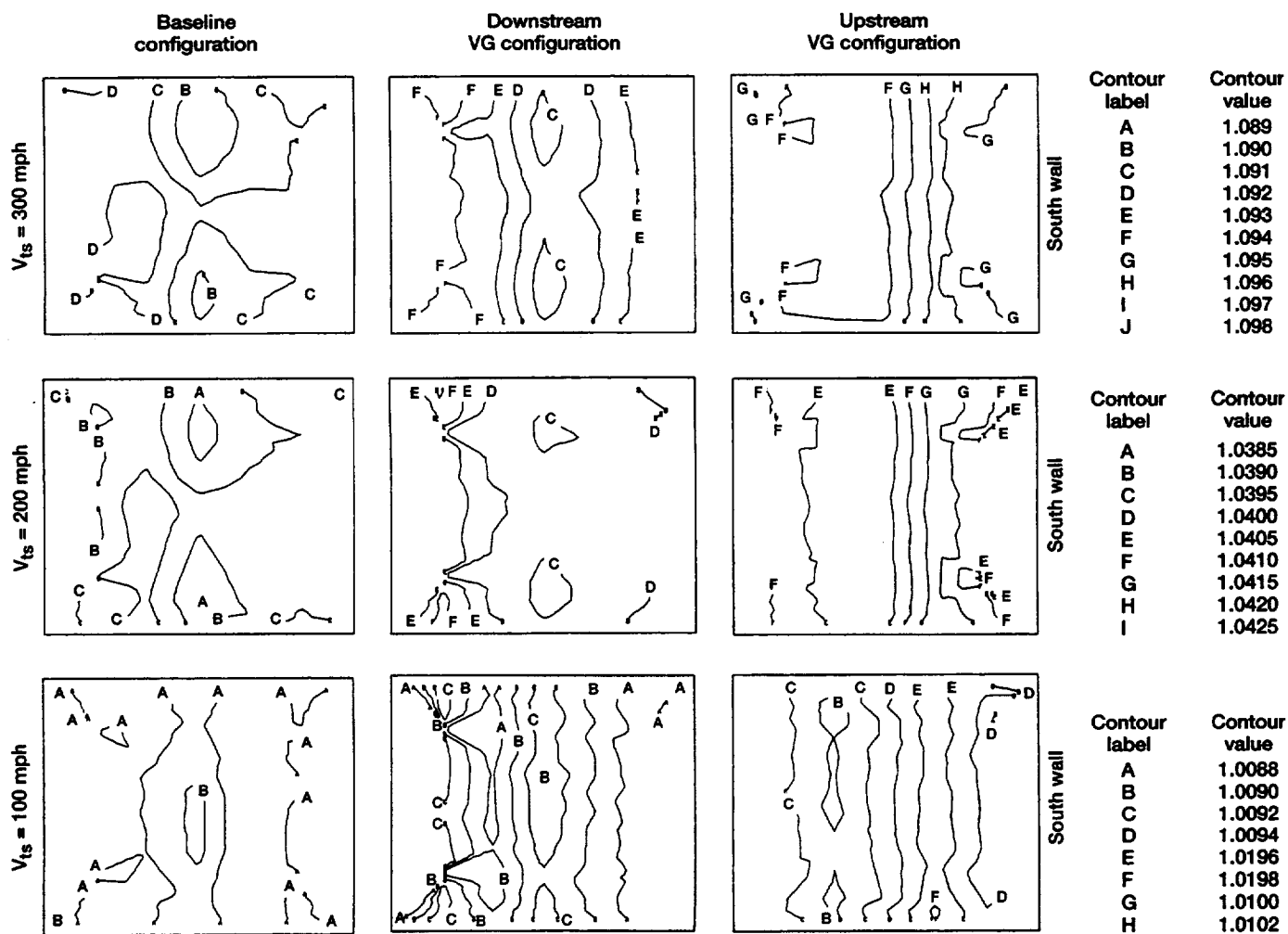


Figure 11.—Contour plots of static pressure survey data collected at the diffuser exit normalized by test section static pressure ($P_s/P_{s,ts}$). (Downstream views.)

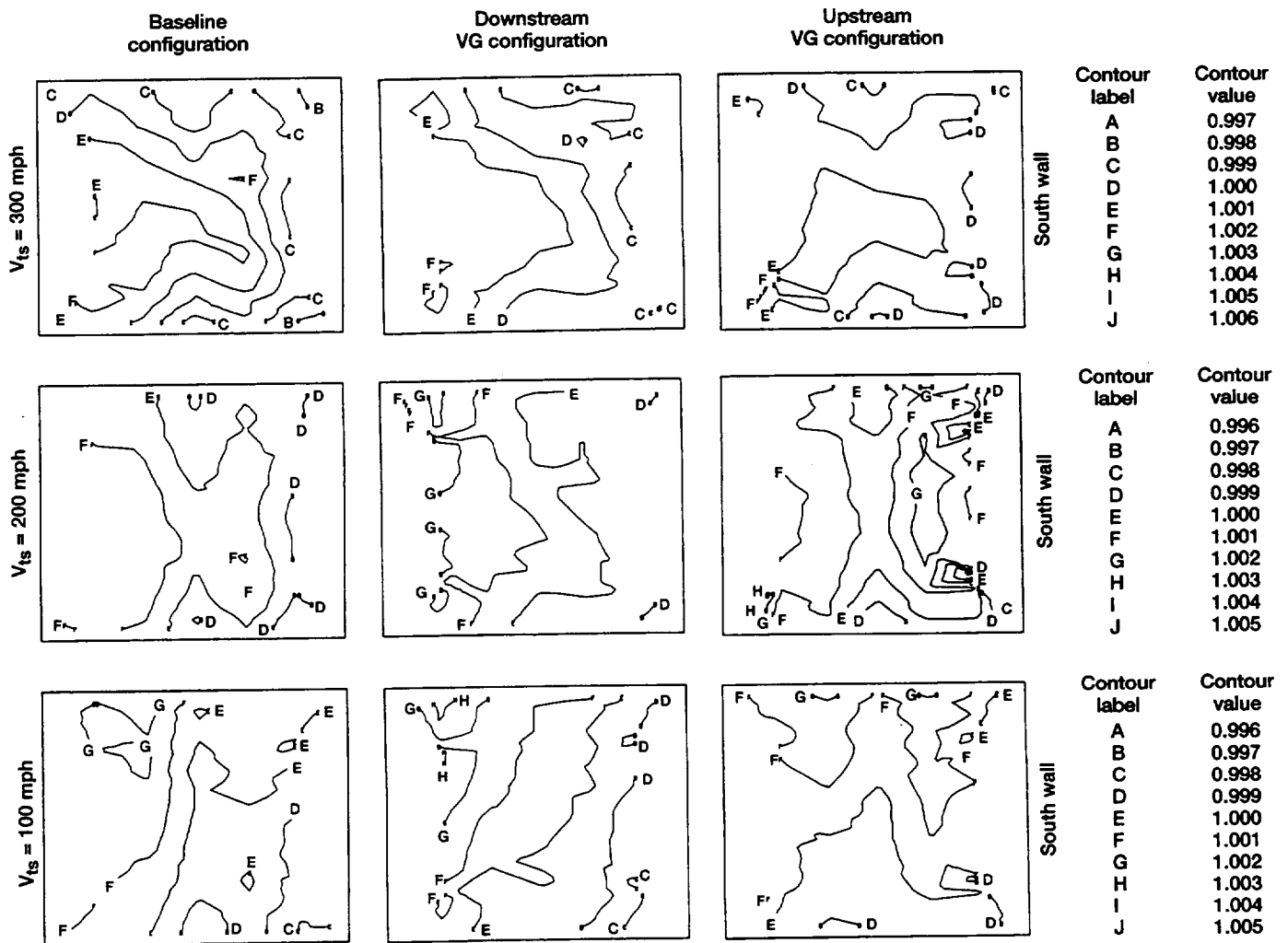


Figure 12.—Contour plots of total temperature survey data collected at the diffuser exit normalized by test section total temperature ($T_0/T_{0,ts}$). (Downstream views.)

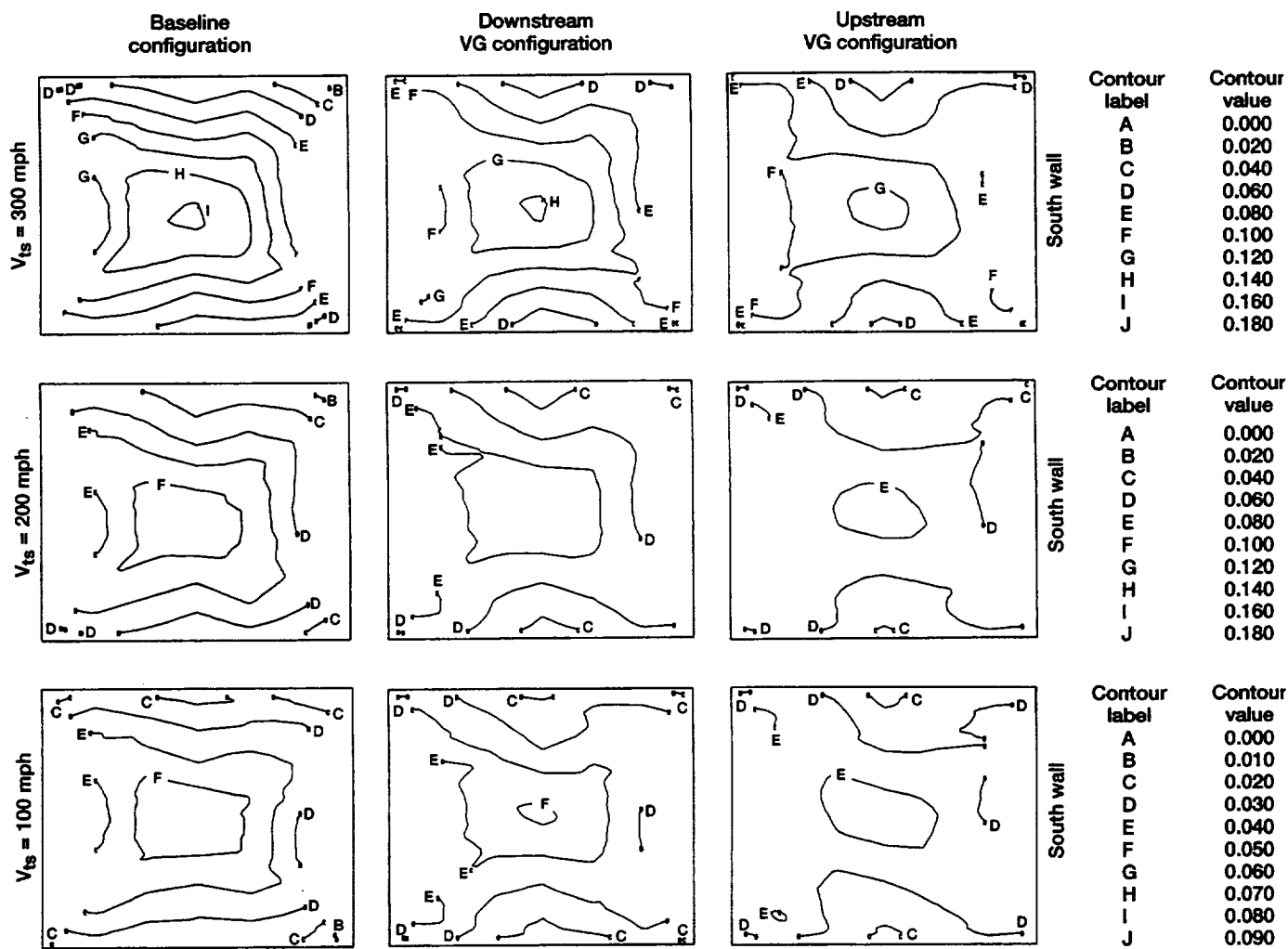


Figure 13.—Contour plots of Mach number data collected at diffuser exit.

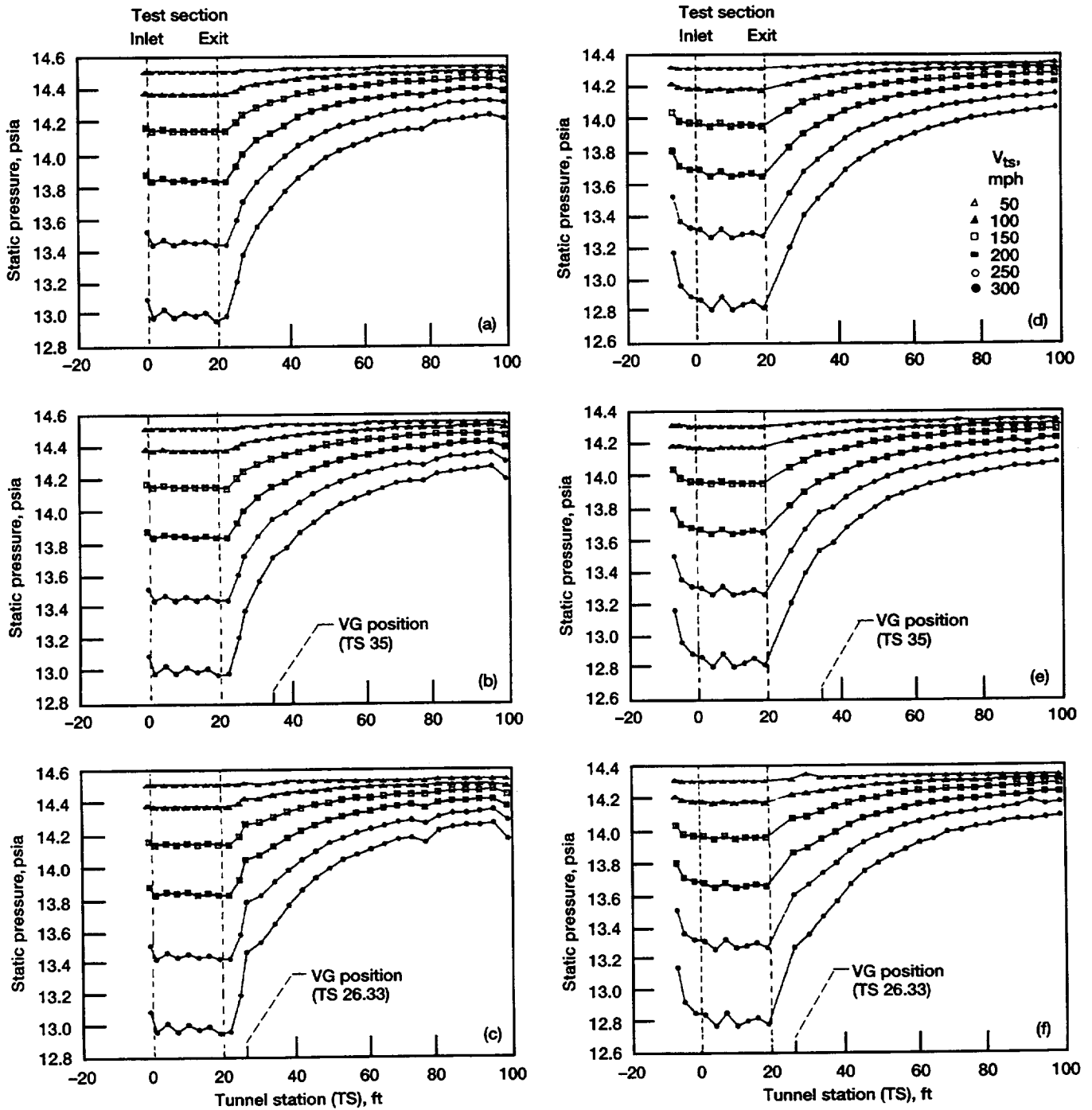


Figure 14.—Static-pressure distributions along the north and south test section and diffuser walls. (a) North wall; baseline configuration. (b) North wall; downstream VG configuration. (c) North wall; upstream VG configuration. (d) South wall; baseline configuration. (e) South wall; downstream VG configuration. (f) South wall; upstream VG configuration.

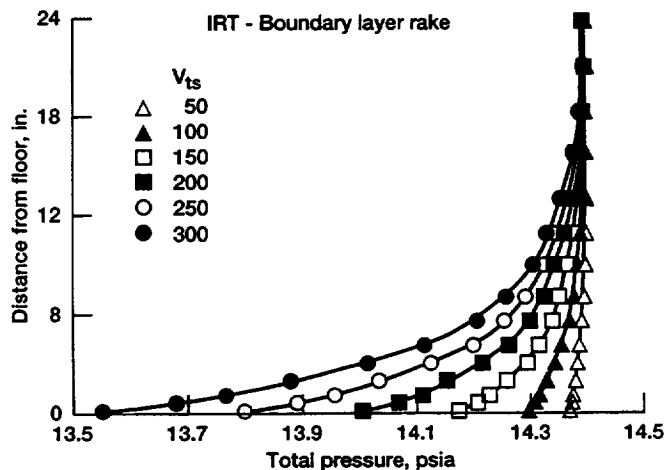


Figure 15.—Boundary-layer distributions (total pressure) made at diffuser inlet (upstream VG configuration).

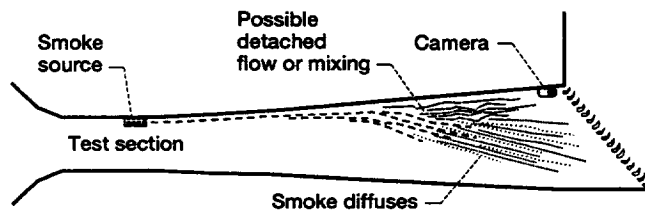


Figure 16.—Diagram of diffuser flow visualization test set up and approximate path of smoke traces.

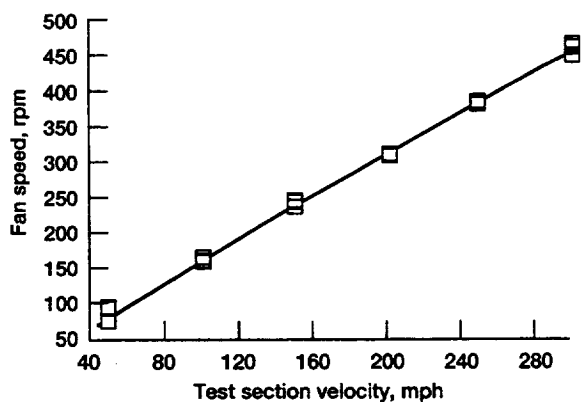


Figure 17.—Drive fan speed required to set corresponding empty test section velocities. Data from a clean (no vortex generators) tunnel.

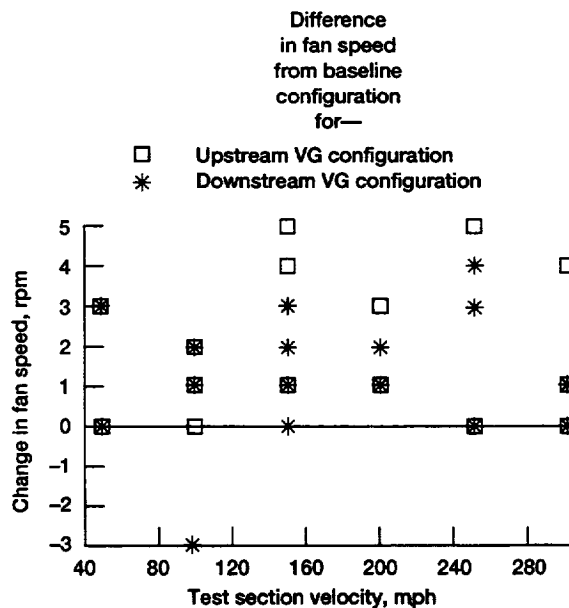


Figure 18.—Difference in drive fan speed to produce empty test section velocities with the vortex generators installed. (Positive numbers indicate decrease in fan speed.)

| REPORT DOCUMENTATION PAGE | | | Form Approved OMB No. 0704-0188 | |
|--|---|---|------------------------------------|--|
| Public reporting burden for this collection of information is estimated to average 1 hour per response, including the time for reviewing instructions, searching existing data sources, gathering and maintaining the data needed, and completing and reviewing the collection of information. Send comments regarding this burden estimate or any other aspect of this collection of information, including suggestions for reducing this burden, to Washington Headquarters Services, Directorate for Information Operations and Reports, 1215 Jefferson Davis Highway, Suite 1204, Arlington, VA 22202-4302, and to the Office of Management and Budget, Paperwork Reduction Project (0704-0188), Washington, DC 20503. | | | | |
| 1. AGENCY USE ONLY (Leave blank) | 2. REPORT DATE January 1994 | 3. REPORT TYPE AND DATES COVERED Technical Memorandum | | |
| 4. TITLE AND SUBTITLE Flow Quality Studies of the NASA Lewis Reserch Center Icing Research Tunnel Diffuser | | 5. FUNDING NUMBERS WU-505-62-84 | | |
| 6. AUTHOR(S) E. Allen Arrington, Mark T. Pickett, and David W. Sheldon | | | | |
| 7. PERFORMING ORGANIZATION NAME(S) AND ADDRESS(ES) National Aeronautics and Space Administration Lewis Research Center Cleveland, Ohio 44135-3191 | | 8. PERFORMING ORGANIZATION REPORT NUMBER E-8051 | | |
| 9. SPONSORING/MONITORING AGENCY NAME(S) AND ADDRESS(ES) National Aeronautics and Space Administration Washington, D.C. 20546-0001 | | 10. SPONSORING/MONITORING AGENCY REPORT NUMBER NASA TM-106311 | | |
| 11. SUPPLEMENTARY NOTES E. Allen Arrington, Sverdrup Technology, Inc., Lewis Research Center Group, 2001 Aerospace Parkway, Brook Park, Ohio 44142, and Mark T. Pickett and David W. Sheldon, NASA Lewis Research Center. Responsible person, David W. Sheldon, (216) 433-8507 | | | | |
| 12a. DISTRIBUTION/AVAILABILITY STATEMENT Unclassified - Unlimited Subject Category 09 | | | 12b. DISTRIBUTION CODE | |
| 13. ABSTRACT (Maximum 200 words) The purpose of this study was to document the airflow characteristics in the diffuser of the NASA Lewis Research Center Icing Research Tunnel and to determine the effects of vortex generators on the flow quality in the diffuser. The results of this study were used to determine how to improve the flow in this portion of the tunnel so that it can be more effectively used as an icing test section and such that overall tunnel efficiency can be improved. The demand for tunnel test time and the desire to test models that are too large for the test section were two of the drivers behind this diffuser study. For all vortex generator configurations tested, the flow quality was improved. | | | | |
| 14. SUBJECT TERMS Wind tunnel; Flow quality; Flow field measurement; Diffuser; Vortex generator | | | 15. NUMBER OF PAGES 18 | |
| | | | 16. PRICE CODE A03 | |
| 17. SECURITY CLASSIFICATION OF REPORT Unclassified | 18. SECURITY CLASSIFICATION OF THIS PAGE Unclassified | 19. SECURITY CLASSIFICATION OF ABSTRACT Unclassified | 20. LIMITATION OF ABSTRACT | |